arXiv:nlin/0001058v1 [nlin.CD] 26 Jan 2000

Applying Blind Chaos Control to Find Periodic Orbits

Daniel T. Kaplan
Department of Mathematics and Computer Science
Macalester College
St. Paul, Minnesota 55105

February 8, 2008

Abstract

Abstract: Analysis of the PPF chaos control method used in biological experiments shows that it can robustly control a wider class of systems than previously believed, including those without stable manifolds. This can be exploited to find the locations of unstable periodic orbits by varying the parameters of the control system.

PACS numbers: 87.10.+e, 05.45.+b, 07.05.Dz

One of the most surprising successes of chaos theory has been in biology: the experimentally demonstrated ability to control the timing of spikes of electrical activity in complex and apparently chaotic systems such as heart tissue [1] and brain tissue [2]. In these experiments, PPF control — a modified formulation of OGY control [3] — was applied to set the timing of external stimuli; the controlled system showed stable periodic trajectories instead of the irregular interspike intervals seen in the uncontrolled system. The mechanism of control in these experiments was interpreted originally as analogous to that of OGY control: unstable periodic orbits riddle the chaotic attractor and the electrical stimuli place the system's state on the stable manifold of one of these periodic orbits.

Alternative possible mechanisms for the experimental observations have been described by Zeng and Glass [4] and Christini and Collins [5]. These authors point out that the controlling external stimuli serve to truncate the interspike interval to a maximum value. When applied, the control stimulus sets the next interval s_{n+1} to be on the line

$$s_{n+1} = \mathcal{A}s_n + \mathcal{C}. \tag{1}$$

We will call this relationship the "control line." Zeng and Glass showed that if the uncontrolled relationship between interspike intervals is a chaotic one-dimensional function, $s_{n+1} = f(s_n)$, then the control system effectively flattens the top of this map and the controlled dynamics may have fixed points or other periodic orbits[4]. Christini and Collins showed that behavior analogous to the fixed-point control seen in the biological experiments can be accomplished even in completely random systems[5]. Since neither chaotic one-dimensional systems nor random systems have a stable manifold, the interval-truncation interpretation of the biological experiments is different than the OGY interpretation. The interval-truncation method differs also from OGY and related control methods in that the perturbing control input is a fixed-size stimulus whose timing can be treated as a continuous parameter. This type of input is conventional in cardiology (e.g., [6]).

In this Letter, we show that the state-trunction interpretation is applicable in cases where there is a stable manifold of a periodic orbit as well as in cases where there are only unstable manifolds. We find that superior control can be achieved by intentionally placing the system's state off of any stable manifold. This suggests a powerful scheme for the rapid experimental identification of fixed points and other periodic orbits in systems where interspike intervals are of interest.

The chaos control in [1] and [2] was implemented in two stages. First, interspike intervals s_n from the uncontrolled, "natural" system were observed. Modeling the system as a function of two variables $s_{n+1} = f(s_n, s_{n-1})$, the location $s^\star$ of a putative unstable flip-saddle type fixed point and the corresponding stable eigenvalue λ_s were estimated from the data.[7] (Since the fixed point is unstable, there is also an unstable eigenvalue λ_u.) The linear approximation to the stable manifold lies on a line given by Eq. 1 with $\mathcal{A} = \lambda_s$ and $\mathcal{C} = (1 - \lambda_s)s^\star$. Second, using estimated values of $\mathcal{A}$ and $\mathcal{C}$, the control system was turned on. Following each observed interval s_n, the maximum allowed value of the next interspike interval was computed as $\mathcal{S}_{n+1} = \mathcal{A}s_n + \mathcal{C}$. If the next interval naturally was shorter than $\mathcal{S}_{n+1}$ no

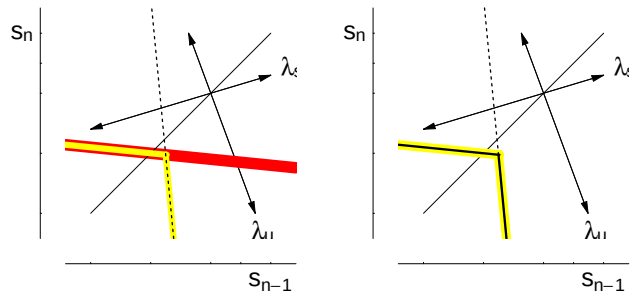

Figure 1: Successive images of the control line for a flip saddle with $\lambda_s = 0.3$, $\lambda_u = -2.7$, $\mathcal{A} = -0.1$, and $x^\star - s^\star = -.75$. Left: the control line is shown as the broad dark gray line. Its image under the natural dynamics is shown as a dashed line; the image under the control dynamics is the bent light gray line. Right: the first image of the control line is replotted. The image of this under the natural dynamics is the dashed line; the image under the control dynamics is the solid line.

control stimulus was applied to the system. Otherwise, an external stimulus was provided to truncate the interspike interval at $s_{n+1} = \mathcal{S}_{n+1}$. [8]

In practice, the values of $s^\star$ and λ_s for a real fixed point of the natural system are known only imperfectly from the data. Insofar as the estimates are inaccurate, the control system does not place the state on the true stable manifold. Therefore, we will analyze the controlled system without presuming that $\mathcal{A}$ and $\mathcal{C}$ in Eq. 1 correspond to the stable manifold.

If the natural dynamics of the system is modeled by $s_{n+1} = f(s_n, s_{n-1})$, the dynamics of the controlled system is given by

$$s_{n+1} = \min \begin{cases} f(s_n, s_{n-1}) & \text{Natural Dynamics} \\ \mathcal{A}s_n + \mathcal{C} & \text{Control Line} \end{cases} \tag{2}$$

We can study the dynamics of the controlled system close to a natural fixed point, $s^\star$, by approximating the natural dynamics linearly [9] as

$$\begin{aligned} s_{n+1} = f(s_n, s_{n-1}) \quad &= \quad (\lambda_s + \lambda_u)s_n - \lambda_s\lambda_u s_{n-1} \\ &\quad\; + s^\star(1 + \lambda_s\lambda_u - \lambda_s - \lambda_u) \end{aligned} \tag{3}$$

Since the controlled system (Eq. 2 is nonlinear even when $f()$ is linear, it is difficult to analyze its behavior by algebraic iteration. Nonetheless, the controlled system can be studied in terms of one-dimensional maps.

Following any interspike interval when the controlling stimulus has been applied, the system's state (s_n, s_{n-1}) will lie somewhere on the control line. From this time onward the state will lie on an image of the control line even if additional stimuli are applied during future interspike intervals.

Figure 1 (left) shows an example of how the dynamics result in a simple one-dimensional map for the case where the natural dynamics have a flip saddle ($\lambda_u < -1$ and $0 < \lambda_s < 1$) and where the control line intersects the line of identity ($s_n = s_{n-1}$) below the natural fixed point $s^\star$. The stable and unstable manifolds are shown as arrows which intersect at the location of the natural fixed point $s^\star$. The control line is shown as a broad dark gray stripe. Its image under the natural dynamics is shown as a thin dashed line. At some points this image is above the control line and is therefore truncated (in the vertical direction) by the control stimulus to be on the control line. Overall, the image of the control line under the controlled dynamics is shown as the broad light gray bent line. In this case, the first, second, and all successive images of the control line are all the same: see Fig 1 (right).

Once the control stimulus has been applied, the dynamics of the controlled system are described by a one-dimensional map: the bent light gray line in Fig. 1. The analysis of the dynamics of this map is straightforward. For the case shown in Fig. 1, the map has a fixed point (where the flat part of the map intersects the line of identity). Near this fixed point, the map is identical to the control line, so the fixed point of the map is also the "controller fixed point,"

$$x^\star = \mathcal{C}/(1 - \mathcal{A})$$

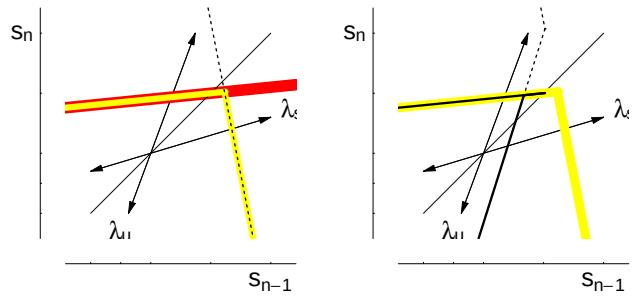

Figure 2: Successive images of the control line for a non-flip saddle: $\lambda_s = 0.3$, $\lambda_u = 2.7$, $\mathcal{A} = -0.1$, $x^\star - s^\star = .5$. (See Fig. 1 for the key.) The stable fixed point of the controlled dynamics is located just to the right of the elbow in the image of the control line.

where the control line intersects the line of identity.

Figure 2 illustrates a more complicated case, a non-flip saddle with $x^\star > s^\star$, where successive images of the control line do not all overlap. In this case, successive images are not identical, but there is still a stable fixed point of the controlled dynamics at $x^\star$.

The stability of the controlled dynamics fixed point and the size of its basin of attraction can be analyzed in terms of the control line and its image. When the previous interspike interval has been terminated by a control stimulus, the state lies somewhere on the control line. If the controlled dynamics are to have a stable fixed point, this must be at the controller fixed point $x^\star$ where the control line intersects the line of identity. However, the controller fixed point need not be a fixed point of the controlled dynamics. For example, if the image of the controller fixed point is below the controller fixed point, then the interspike interval following a stimulus will be terminated naturally.

For the controller fixed point to be a fixed point of the controlled dynamics, we require that the natural image of the controller fixed point be at or above the controller fixed point. One such situation, for the flip saddle, is illustrated in Fig. 1 where it can be seen [10] that the natural image of a neighborhood of the control line near $x^\star$ is above the control line. Thus the dynamics of the controlled system, close to $x^\star$, are given simply by

$$s_{n+1} = \mathcal{A} s_n + \mathcal{C}$$

The fixed point of these dynamics is stable so long as $-1 < \mathcal{A} < 1$. In the case of a flip saddle, we therefore have a simple recipe for successful state-truncation control: position $x^\star$ below the natural fixed point $s^\star$ and set $-1 < \mathcal{A} < 1$.

Fixed points of the controlled dynamics can exist for natural dynamics other than flip saddles. This can be seen using the following reasoning: Let ξ be the difference between the controller fixed point and the natural fixed point: $s^\star = x^\star + \xi$. Then the natural image of the controller fixed point can be found from Eq. 3 to be

$$\begin{aligned} s_{n+1} &= (\lambda_s + \lambda_u)x^\star - \lambda_s\lambda_u x^\star \\ &\quad + (1 + \lambda_s\lambda_u - \lambda_s - \lambda_u)(x^\star + \xi) \end{aligned} \tag{4}$$

The condition that

$$s_{n+1} \geq x^\star \tag{5}$$

will be satisfied depending only on λ_s, λ_u, and $\xi = s^\star - x^\star$. In the case represented in Fig. 1, where $\xi < 0$ and $\lambda_u < -1$, the condition $s_{n+1} > x^\star$ will be satisfied for any $\lambda_s < 1$. This means that for any flip saddle, so long as $x^\star < s^\star$, the point $x^\star$ will be a fixed point of the controlled dynamics and will be stable so long as $-1 < \mathcal{A} < 1$.

Equations 4 and 5 imply that control can lead to a stable fixed point for any type of fixed point except those for which both λ_u and λ_s are greater than 1 (so long as $-1 < \mathcal{A} < 1$). Since the required relationship between $x^\star$ and $s^\star$ for a stable fixed point of the controlled dynamics depends on the eigenvalues, it is convenient to divide the fixed points into four classes, as given in Table 1

For example, for the non-flip saddle shown in Fig. 2, the natural image of the control line at $x^\star$ is above $x^\star$. Thus, the controlled image will be truncated (vertically) to be identical to $x^\star$ and therefore the

Type of FP	λ_u	λ_s	$x^\star$ Locat.
Flip saddle	$\lambda_u < -1$	$-1 < \lambda_s < 1$	$x^\star < s^\star$
Saddle	$\lambda_u > 1$	$-1 < \lambda_s < 1$	$x^\star > s^\star$
Single-flip repeller	$\lambda_u > 1$	$\lambda_s < -1$	$x^\star > s^\star$
Double-flip repeller	$\lambda_u < -1$	$\lambda_s < -1$	$x^\star < s^\star$
Spiral (complex λ)	$\lvert\lambda_u\rvert > 1$	$\lvert\lambda_s\rvert > 1$	$x^\star < s^\star$

Table 1: Cases which lead to a stable fixed point for the controlled dynamics. In all cases, it is assumed that $|\mathcal{A}| < 1$. (For the cases where $\lambda_s < -1$, the subscript s in λ_s is misleading in that the corresponding manifold is unstable. For the spiral, there is no stable manifold.)

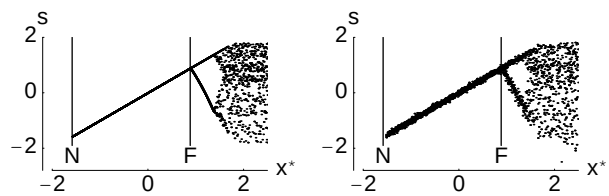

Figure 3: Bifurcation diagrams for the truncation controlled Henon map. Left: No noise. Right: Dynamical noise added (N(0,0.05)).

controller fixed point is also a fixed point of the controlled dynamics. This will be stable for $-1 < \mathcal{A} < 1$, but with a finite basin of attraction.

Beyond the issue of the stability of the fixed point of the controlled dynamics, there is the question of the size of the fixed point's basin of attraction. Although the local stability of the fixed point is guaranteed for the cases in Table 1 for $-1 < \mathcal{A} < 1$, the basin of attraction of this fixed point may be small or large depending on $\mathcal{A}$, $\mathcal{C}$, $s^\star$, λ_u and λ_s. For the case of Fig. 1, the basin is finite when $|\lambda_s + \lambda_u - \lambda_s\lambda_u/\mathcal{A}| > 1$. In the case of Fig. 2, and for non-flip repellers generally, any initial condition that is mapped to below the λ_s eigenvector will receed away from $x^\star$. [12]

The endpoints of the basin of attraction can be derived analytically[12]. The size of the basin of attraction will often be zero when $\mathcal{A}$ and $\mathcal{C}$ are chosen to match the stable manifold of the natural system. Therefore, in order to make the basin large, it is advantageous intentionally to misplace the control line and to put $x^\star$ in the direction indicated in Table 1. In addition, control may be enhanced by setting $\mathcal{A} \neq \lambda_s$, for instance $\mathcal{A} = 0$.

If the relationship between $x^\star$ and $s^\star$ is reversed from that given in Table 1, the controlled dynamics will not have a stable fixed points. To some extent, these can also be studied using one-dimensional maps. The flip saddle and double-flip repeller can display stable period-2 orbits and chaos. For the non-flip saddle and single-flip repeller, control is unstable when $x^\star < s^\star$.

The fact that control may be successful or even enhanced when $\mathcal{A}$ and $\mathcal{C}$ are not matched to λ_s and $s^\star$ suggests that it may be useful to reverse the experimental procedure often followed in chaos control. Rather than first identifying the parameters of the natural unstable fixed points and then applying the control, one can blindly attempt control and then deduce the natural dynamics from the behavior of the controlled system. This use of PPF control is reminiscent of pioneering studies that used periodic stimulation to demonstrate the complex dynamics of biological preparations[11].

As an example, consider the Henon map:

$$s_{n+1} = 1.4 + 0.3 s_{n-1} - s_n^2$$

This system has two distinct fixed points. There is a flip-saddle at $s^\star = 0.884$ with $\lambda_u = -1.924$ and $\lambda_s = 0.156$ and a non-flip saddle at $s^\star = -1.584$ with $\lambda_u = 3.26$ and $\lambda_s = -0.092$. In addition, there is an unstable flip-saddle orbit of period 2 following the sequence $1.366 \to -0.666 \to 1.366$. There are no real orbits of period 3, but there is an unstable orbit of period 4 following the sequence $.893 \to .305 \to 1.575 \to -.989 \to .893$. These facts can be deduced by algebraic analysis of the equations.

In an experiment using the controlled system, the control parameter $x^\star = \mathcal{C}/(1-\mathcal{A})$ can be varied. The theory presented above indicates that the controlled system should undergo a bifurcation as $x^\star$ passes through $s^\star$. Figure 3 shows the bifurcation diagram for the controlled Henon system (with $\mathcal{A} = 0$). For each value of $x^\star$, the controlled system was iterated from a random initial condition and the values of s_n plotted after allowing a transient to decay[13]. A bifurcation from a stable fixed point to a stable period 2 as $x^\star$ passes through the flip-saddle value of $s^\star = 0.884$. A different type bifurcation occurs

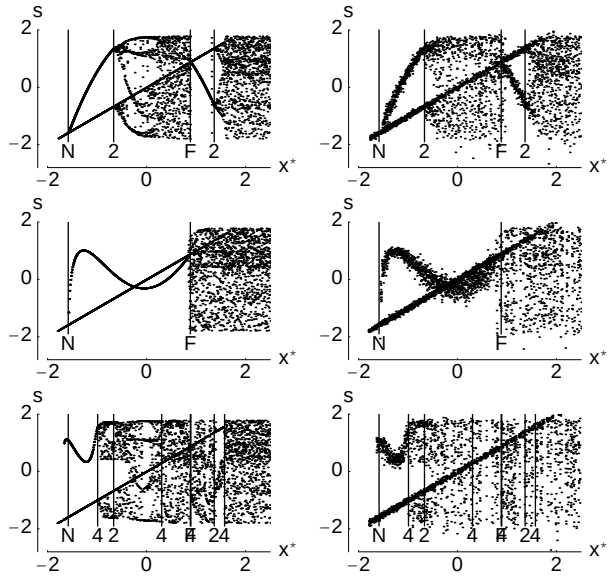

Figure 4: Bifurcation diagrams for the truncation controlled Henon map where truncation control is activated only every second (top), third (middle), or fourth (bottom) iteration. Left: No noise. Right: Dynamical noise added (N(0,0.05)). The locations of the true fixed points are marked with vertical lines: F flip-saddle; N non-flip saddle; 2 period-2 orbit; 4 period-4 orbit.

at the non-flip saddle fixed point at $s^\star = -1.584$. To the left of the bifurcation point, the iterates are diverging to $-\infty$ and are not plotted.

Adding gaussian dynamical noise (of standard deviation 0.05) does not substantially alter the bifurcation diagram, suggesting that examination of the truncation control bifurcation diagram may be a practical way to read off the location of the unstable fixed points in an experimental preparation.

By activating the truncation control after every second, third or fourth iteration, it is possible to find periodic orbits of period 2, 3, and 4 respectively. The bifurcation diagrams are shown in Fig. 4. The location of the period-2 orbits can be clearly discerned even in the presence of noise. No period-3 orbit is indicated. Noise obscures the location of all but one of the period-4 points.

Unstable periodic orbits can be difficult to find in uncontrolled dynamics because thre is typically little data near such orbits. Application of PPF control, even blindly, can stabilize such orbits and dramatically improve the ability to locate them. This, and the robustness of the control, may prove particularly useful in biological experiments where orbits may drift in time as the properties of the system change. [14]

We would like to acknowledge helpful conversations with Thomas Schreiber and Leon Glass.

References

[1] A. Garfinkel, M.L. Spano, W.L. Ditto, J.N. Weiss Science 257:1230-1235 (1992)

[2] S.J. Schiff, K. Jerger, D.H. Duong, T. Chang, M.L. Spano and W.L. Ditto, Nature (London) **370**, 614 (1994)

[3] E. Ott, C. Grebogi, and J.A. Yorke Phys. Rev. Lett. 64:1196-1199 (1990)

[4] L. Glass and W. Zeng, Int. J. Bifurcation and Chaos **4**:1061 (1994)

[5] D.J. Christini and J.J. Collins, Phys. Rev. Lett. **75**:2782-2785 (1995)

[6] K. Hall et al. PRL 78(23):4518-4521:63-75 (1997)

[7] A method for identifying unstable fixed points from time series data is described in P. So et al., PRE 55(5):5398-5417 (1997). The relationship between the underlying continuous-time dynamics and the discrete-time map of interspike intervals is discussed in T. Sauer in C.D. Cutler and D.T. Kaplan, eds, Nonlinear Dynamics and Time Series, Fields Inst. Comm. 11 American Mathematical Society, 63-75, (1997) and in M. Ding and W. Yang PRE 55(3):2397-2402 (1997)

[8] This truncation is reminiscent of the mythical Greek inkeeper Procrustes. Travellers too tall for his bed were truncated to fit in a rather gruesome manner. Although PPF originally was intended to stand for "Proportional Perturbation Feedback," the nonlinear all-or-nothing nature of the perturbation suggests that an alternative expansion is more appropriate: "Procrustean Perturbation Feedback."

[9] Eq. 3 is simply the linear equation $s_{n+1} = as_n + bs_{n-1} + c$ with a, b, and c set to give eigenvalues λ_s and λ_u and fixed point $s^\star$.

[10] The image of a single point on the control line can be found graphically using the cobweb method. From the point, trace horizontally to the line of identity, then vertically to the image of the control line. If following the natural dynamics, trace to the natural image. If following the controlled dynamics, trace toward the natural image but stop at the control line if that is below the natural image.

[11] M.R. Guevara, L. Glass, A. Shrier, Science **214**:1350-53 (1981)

[12] Details will be provided in a subsequent communication.

[13] No attempt was made to wait until the system state naturally approached a putative fixed point. The truncation control was active at all time. The decay of the transient typically took only a few iterations.

[14] An example of such drifts and their influence on control is found in K. Hall et al. (ibid) and D.J. Gauthier and J.E.S. Socolar, Phys. Rev. Let., Vol. 79, p. 4938 (1997).